

Article

Greenhouse Effect and the IR Radiative Structure of the Earth's Atmosphere

Ferenc Miskolczi

3 Holston Lane, Hampton, VA 23664, USA

E-Mail: fmiskolczi@cox.net; Tel.: 757-851-7505

Received: / Accepted: / Published:

Abstract: There are accumulating evidences that the greenhouse effect in the Earth's atmosphere is not a 'free' parameter and anthropogenic global warming (AGW) estimates based on the classic greenhouse theory and CO₂ doubling experiments (usually conducted by general circulation models) are totally wrong. Based on large number of observed atmospheric thermal and humidity structures and global scale simulations of the true greenhouse gas absorption properties of the atmosphere it is shown that the global average clear sky greenhouse effect is constant. The observed true infrared optical thickness of the clear atmosphere is 1.87 and this value proved to be very stable in the last 61 years. With the help of the observed relationships among the radiative flux components and the association of those relationships with known fundamental physical laws new structural equations of the global radiation field were established. The theoretically predicted IR optical thickness is fully consistent with, and supporting the observed value of 1.87. Apparently, the infrared atmospheric absorption of our water-rich planet is entirely controlled by the dynamics of the system. Since all essential flux density components are scaled with the absorbed solar radiation, surface temperature changes are only possible via the changes in the short wave absorption-reflection or the long wave emission characteristics of the surface-atmosphere system.

Keywords: greenhouse effect, radiative transfer, global warming.

1. Introduction

From time to time one may encounter with articles in main stream scientific journals from recognized scientists about the greenhouse effect and global warming. From Lacis et al. [1] we learn that, assuming global energy balance, the absorption and re-emission of the surface upward infrared (terrestrial) radiation by greenhouse gases is the reason of the $G = \sigma t_G^4 - \sigma t_E^4 = S_G - OLR = 150 \text{ Wm}^{-2}$ observed greenhouse warming. Here G is the greenhouse factor, $\sigma = 5.67 \times 10^{-8} \text{ Wm}^{-2}\text{K}^{-4}$ is the Stefan-Boltzmann constant, $t_G = 288 \text{ K}$ is the ground temperature, and $t_E = 255 \text{ K}$ is the effective planetary temperature computed from the total short wave (SW) solar radiation absorbed by the system, F^o . In case of a perfectly black surface S_G is the surface upward radiation. For non-black surfaces the upward radiation is defined by the skin temperature: $S_U = \sigma t_S^4 = \varepsilon_G \sigma t_G^4 \leq S_G$, where ε_G is the surface flux emissivity. Global energy (or radiation) balance means that the long wave (LW) outgoing radiation, OLR equal to F^o . In [1] it is also stated that - although the H_2O is the most powerful greenhouse gas - the CO_2 controls the atmospheric greenhouse effect. Interestingly the role of the cloud cover in the climate system is discussed as if it were just another kind of greenhouse gas.

According to Pierrehumbert [2] due to well established energy balance principles increased atmospheric CO_2 will inevitably followed by increased greenhouse effect. The most popular global energy balance schemes were published by Kiehl and Trenberth [3] and Trenberth et al. [4]. In [3,4] the global average terrestrial radiation field was modeled by using a version of the US Standard Atmosphere 76 in which - in order to match with ERBE observations [5] - the H_2O column amount was reduced from 1.42 to 1.26 precipitable cm (prcm). In [3] the all-sky and clear-sky greenhouse factors were reported as 155 and 135 Wm^{-2} subsequently.

For a numerical example in Fig 1 the clear-sky greenhouse effect is demonstrated for the planets Mars and Earth. The computations were performed for the US standard atmosphere used in [4] and for an average Martian atmosphere used in [6]. In the semi-transparent planetary atmospheres above the OLR s were computed as the sums of the transmitted flux density, S_T , and the atmospheric upward emittance, E_U . Accurate line-by-line (LBL) flux densities were obtained by using the High-resolution Atmospheric Radiative Transfer Code, (HARTCODE), [7, 8, 9]. Apparently the planetary greenhouse factors are not known with very high degree of accuracy. In [1] G is 5 Wm^{-2} less than the one in [3], and according to Fig. 1 our clear-sky G is about 5 Wm^{-2} higher than the one reported in [3]. Such differences in the radiative fluxes may be translated to about 1.3 K and 1.0 K uncertainty in t_E and t_G correspondingly. Compared to the observed $\sim 0.012 \text{ K/year}$ positive trend in the surface temperature in the last 61 years [10] and the recent skills of the GCMs in predicting the changes in G for CO_2 doubling the proof of the CO_2 greenhouse effect based anthropogenic global warming, (AGW) is not imminent.

In the next example we wish to point to serious theoretical deficiencies in the common practice of using the greenhouse factor as a measure of the IR atmospheric (greenhouse gas) absorption. In our comparison we clearly show that the greenhouse effect represented by the G factor is not consistent

Figure 1. The greenhouse factors are the flux density differences computed by the Stefan-Boltzmann law for the t_G and t_E temperatures (shaded areas). The OLR s (thin solid lines) were computed using HARTCODE with 1.0 cm^{-1} spectral resolution.

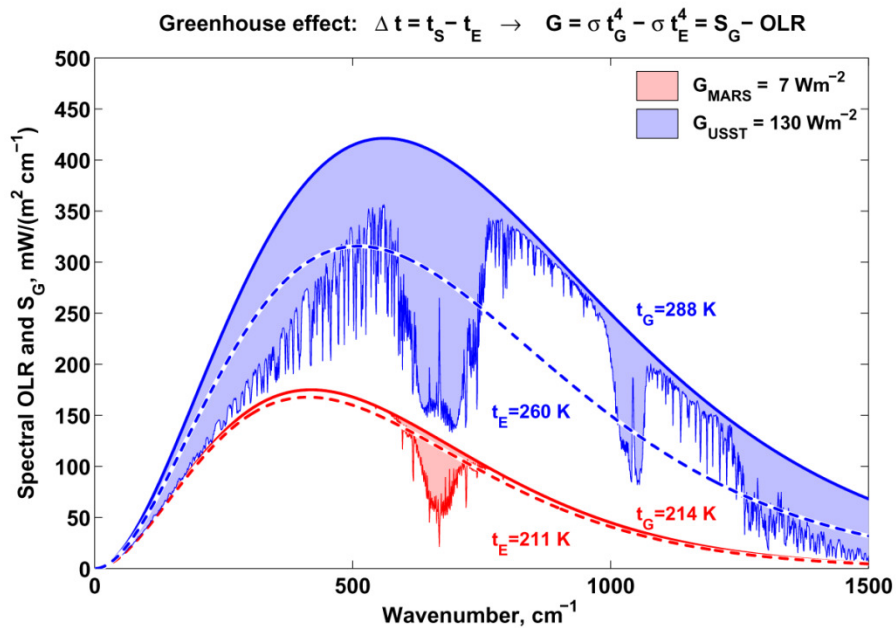
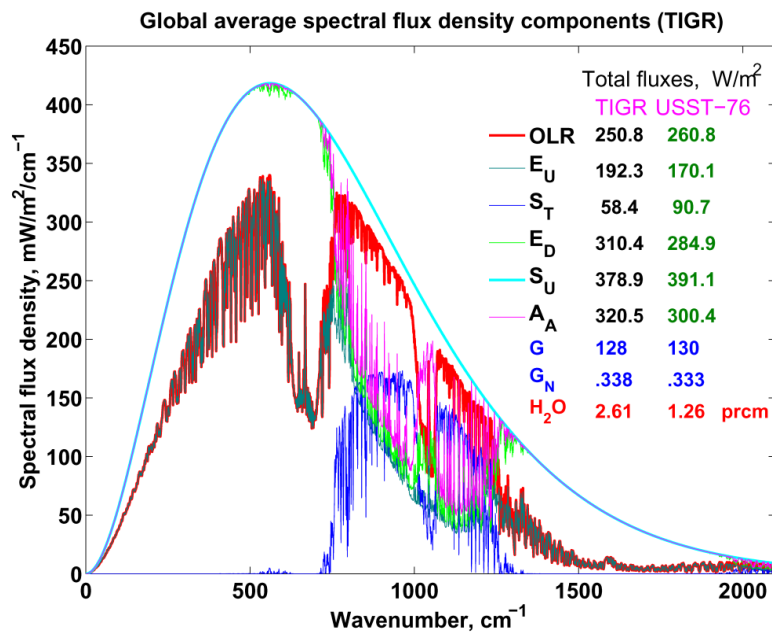


Figure 2. The clear-sky greenhouse factors and the $G_N = G/S_U$ normalized greenhouse factors are practically the same for both atmospheric structures. E_D and A_A are downward atmospheric emittance and the absorbed surface upward radiation.



with statements that link the increased greenhouse gas content of the atmosphere to increased IR absorption. From the well known TIGR 2 radiosonde archive [11] a global average atmospheric structure was constructed in [9]. In Fig. 2 radiative flux density components, greenhouse factors, and the H₂O column amounts of the average TIGR 2 profile and the modified USST 76 profile are presented. Note, that the H₂O column amounts in the two profiles are dramatically different. In the above example the greenhouse factor is not sensitive to doubled water vapor amount in the TIGR profile. AGW and IPCC experts or GCM modelers may think about the question: Apparently the greenhouse effect represented by the G factor or G_N is not sensitive to the atmospheric water vapor content, then why to bother with the H₂O feedback (caused by the CO₂ initial greenhouse warming) ?

Considering the above theoretical problem and the permanent failure of the most sophisticated GCMs in predicting the magnitude of the global warming, one should admit, that the real nature of the greenhouse effect is not known. The governing mechanisms of IR absorption properties of the global average atmosphere were never studied with sufficient details. In any serious greenhouse studies the knowledge of the functional dependence of the global average IR flux optical depth, τ_A on the greenhouse gas (GHG) concentrations, and the surface temperatures are absolutely necessary. The flux optical depth, flux absorption, A , and flux transmittance, T_A , are defined by the next relationships: $S_T = S_U(1-A) = S_U T_A = S_U \exp(-\tau_A)$. Except in [6,8] there are no published data available on the theoretical surface temperature - flux optical depth relationship for semi-transparent atmospheres. The obvious reason why the scientific community did not present such results is twofold.

The first is the lack of a suitable greenhouse theory which is based on purely the known fundamental laws of nature. Apart from the fact, that the use of GCMs for studying large scale climate change is conceptually wrong (fundamentally stochastic processes cannot be studied by a deterministic model), the GCMs with their ad-hoc feedback processes are not representing the physics and the true nature of the greenhouse effect. It is known for a long time that climate change is controlled by the net radiative fluxes at the top and bottom boundaries of the system. The global average state of the atmosphere - sometimes called global average climate - is governed by the laws that controls the flow of the global average radiative fluxes at the boundaries. Although GCMs are not the proper tools for long term climate change studies, once the global constraints on the average radiative flux components are known then the GCMs might have a role in evaluating regional or smaller scale responses of the climate system.

The second reason is rather technical, and related to the accurate computation of the flux optical depth. According to a recent statement of Ramanathan and Inamdar [12] the three dimensional characterization of the radiative heating rates from equator to pole using the line-by-line approach is impractical. This view suggests to sacrifice accuracy - by using band models - in global scale radiative transfer computations, where it is most needed. Probably this rather simple-minded view is the reason why in recent textbooks extended parts are devoted to popularize 'ancient' band model techniques, see for example in Pierrehumbert [13]. Unfortunately the fact is that there are no publicly available LBL codes for accurate computations of the true IR flux optical depth.

In the next sections we give an overview of the of the numerical computations of the accurate flux optical depth, present computational results of observed radiative flux density relationships for the planets Earth and Mars, identify and develop the theoretical relationships consistent with the observations and give a new view of the planetary greenhouse effect.

2. The True IR Optical Depth of the Atmosphere

In astrophysics - for the different kind of radiative transfer problems - there are different kinds of definitions for the mean optical depth (or mean opacity). They are the Rosseland, Planck and Chandrasekhar means, and they are in fact different kind of weighted average absorption coefficients. The relevant physical quantity necessary for the computation of the true atmospheric IR absorption is the Planck-weighted greenhouse-gas optical thickness τ_A . The numerical computation of this quantity for a layered spherical refractive atmosphere may be found in Miskolczi [6, 9]. In our definition τ_A is computed from the spectral hemispheric transmittance and therefore represents the true spectral feature of the infrared absorption coefficient. We emphasize that τ_A is not a weighted absorption coefficient in the sense of the usual Planck mean opacity. τ_A is a newly defined physical quantity, and one may not find any reference in the literature to its computational techniques. The existence of the large and organized absorption line catalogues [13, 14], and the development of the high speed computers and LBL computational techniques are the reasons of the above definition of τ_A . Only a full blown LBL radiative transfer code is able to compute the accurate true atmospheric IR flux optical depth. In short, τ_A may be expressed as:

$$\tau_A = -\ln \left[\frac{S_T}{S_U} \right] = -\ln \left[\frac{1}{\sigma t_A^4} \sum_{j=1}^M \pi B(\Delta \nu_j, t_A) \sum_{k=1}^K w^k \bar{T}_A(\Delta \nu_j, \mu^k) \right], \quad (1)$$

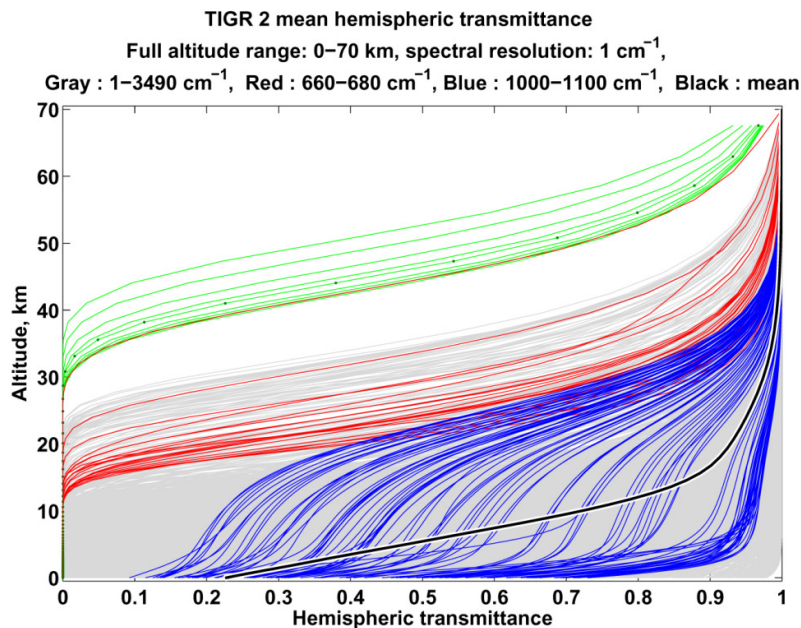
where $M = 3490$ is the total number of spectral intervals, $K = 9$ is the total number of streams, t_A is the surface temperature, B is the Planck function, σ is the Stefan-Boltzmann constant, and w^k is the hemispheric integration weight associated with the k^{th} direction (stream). $\bar{T}_A(\Delta \nu_j, \mu^k)$ is the directional mean transmittance over a suitable short wave number interval:

$$\bar{T}_A(\Delta \nu_j, \mu^k) = \frac{1}{\Delta \nu_j} \int_{\Delta \nu_j} \exp \left[-\sum_{l=1}^L \sum_{i=1}^N \left[c^{i,l} + k_v^{i,l} \right] \frac{u^{i,l}}{\mu^{l,k}} \right] d\nu, \quad (2)$$

where $\mu^{l,k} = \cos(\theta^{l,k}) / dz^l$ and $\theta^{l,k}$ is the local zenith angle of a path segment, $c^{i,l}$ and $k_v^{i,l}$ are the contributions to the total monochromatic absorption coefficient from the continuum type absorptions and all absorption lines relevant to the i^{th} absorber and l^{th} layer respectively. The vertical geometrical layer thickness is dz^l . $N = 11$ is the total number of major absorbing molecular species and $L = 150$ is

the total number of the homogeneous atmospheric layers (shells). In Eqn. (2) the wave number integration is performed numerically by 5th order Gaussian quadrature over a wave number mesh structure of variable length. At least $\Delta\nu_j \approx 1 \text{ cm}^{-1}$ spectral resolution is required for the accurate Planck weighting. From Eqn. (1) follows the usual form of the transmitted and absorbed part of the surface upward radiation. Eqs. (1,2) with the required spherical refractive ray-tracking algorithms are implemented into HARTCODE and facilitate the accurate partition of the OLR to its S_T and E_U components. Unfortunately theoretically no instrument can be devised to measure the monochromatic or spectral S_T^v and E_U^v quantities separately. Since the above radiative components cannot be measured by any airborne or satellite spectrometer this is an essential improvement in the numerical computations of the true IR atmospheric absorption. In Fig. 3 computed hemispheric transmittances from Eq. (2) are presented for the GAT profile and for down looking geometry. In [8, p.233, Eq. (5)] we introduced the atmospheric transfer, $f(\tau_A)$, and greenhouse, $g(\tau_A)$, functions by the next definition: $f = 1 - g = 2/(1 + \tau_A + T_A)$. For an atmospheric air column in radiative balance it was shown that $f = OLR/S_U$ and g is equivalent with the normalized greenhouse factor, G_N [6].

Figure 3. HARTCODE spectral hemispheric transmittances in the $1\text{--}3490 \text{ cm}^{-1}$ spectral range. For the hemispherical integration 9 viewing angles were applied. With 3.21×10^5 vertical optical thickness the 668 cm^{-1} interval exhibits the strongest absorption. For this spectral interval the directional transmittances are also plotted (with green lines). The small black dots belong to the 53.13° isotropic angle and - compared to the red line - indicate considerable error in the widely used isotropic approximation.



One must remember that the so called broad band window radiation is not an adequate quantity to represent the true transmitted surface radiation. To make use of the global average satellite measured broadband window radiation in global radiative budget estimates the data should be corrected (or

calibrated) with global average atmospheric absorption data of the highest accuracy. In Fig. 2 we presented true computed clear-sky transmitted flux densities for the global average TIGR 2 (GAT) and the USST 76 atmospheres. The 32 Wm^{-2} difference in S_T is large enough to raise the question of the quality of the Kiehl-Trenberth [3,4] global energy budget. Although the USST 76 atmosphere could be a good representation of an average mid-latitude atmospheric structure the use of this atmosphere in global energy budget assessments is a serious mistake.

It is time for the IPCC to recognize that no consensus in global warming issues can exist without a declared and accepted standard global average atmosphere. The total IR absorption of such an atmosphere must be computed for the most realistic chemical or GHG composition of the atmosphere and with the highest accuracy. All GHG perturbation studies should be referenced to the absorption and optical thickness of this standard atmosphere.

2. Input Data Sets

Realistic vertical global average thermal and humidity structures may be obtained from readily available climatological radiosonde archives. In this study the GAT global average structure was constructed from the TIGR 2 archive containing 1761 weather balloon observations. An updated version of the TIGR database (known as the TIGR 2000 archive) containing 2311 soundings [15] is also available. The locations, meridional, and annual distributions of the two archives are presented in Fig. 4. Both archives contain prohibitively large number of soundings for LBL computations. After some regional and seasonal grouping we selected a subset of 228 profiles, see Fig. 5. In the subset the statistical characteristics of the original data set were preserved.

For studying the possible long term changes in the global average τ_A (due to changes in GHG content of the atmosphere) the TIGR 2 archive is not suitable. The publicly available longest time series of annual mean vertical temperature and humidity structures may be obtained from the NOAA Earth System Research Laboratory [10] time series data archive. This archive - known as the NCEP/NCAR R1 data set - covers the 1948-2008 time period. A quick look at the data immediately shows that the range of the variations in the annual mean over the 61 years are very small: $58.87 \text{ atm-cm}_{\text{STP}}$ in CO_2 , -0.0169 prcm in H_2O , and 0.687 K in surface temperature. The related year-to-year changes are also very small, 0.35 \%/year in c , 0.0106 \%/year in u , and 0.0039 \%/year in t_A . Here c , u , and t_A stand for the CO_2 and H_2O column amounts and for the surface air temperature, subsequently. Obviously, there is strict and high requirement on the sensitivity and numerical accuracy of the computed fluxes and flux optical thicknesses.

In the flux density computations for the Martian atmospheres we used 18 dust free standard atmospheric structures [6]. In the atmospheric composition only the O_3 , H_2O , CO , N_2 and CO_2 volume mixing ratio profiles were considered.

Figure 4. The TIGR climatological datasets. Detailed comparisons show that the global average TIGR 2 surface air temperature is 0.28 K colder and the vertical air column contains 0.1 prcm (about 3 %) less H₂O. Since in the TIGR 2000 version the vertical H₂O structure was artificially modified (the upper tropospheric humidity was increased) we decided to use the original TIGR 2 archive.

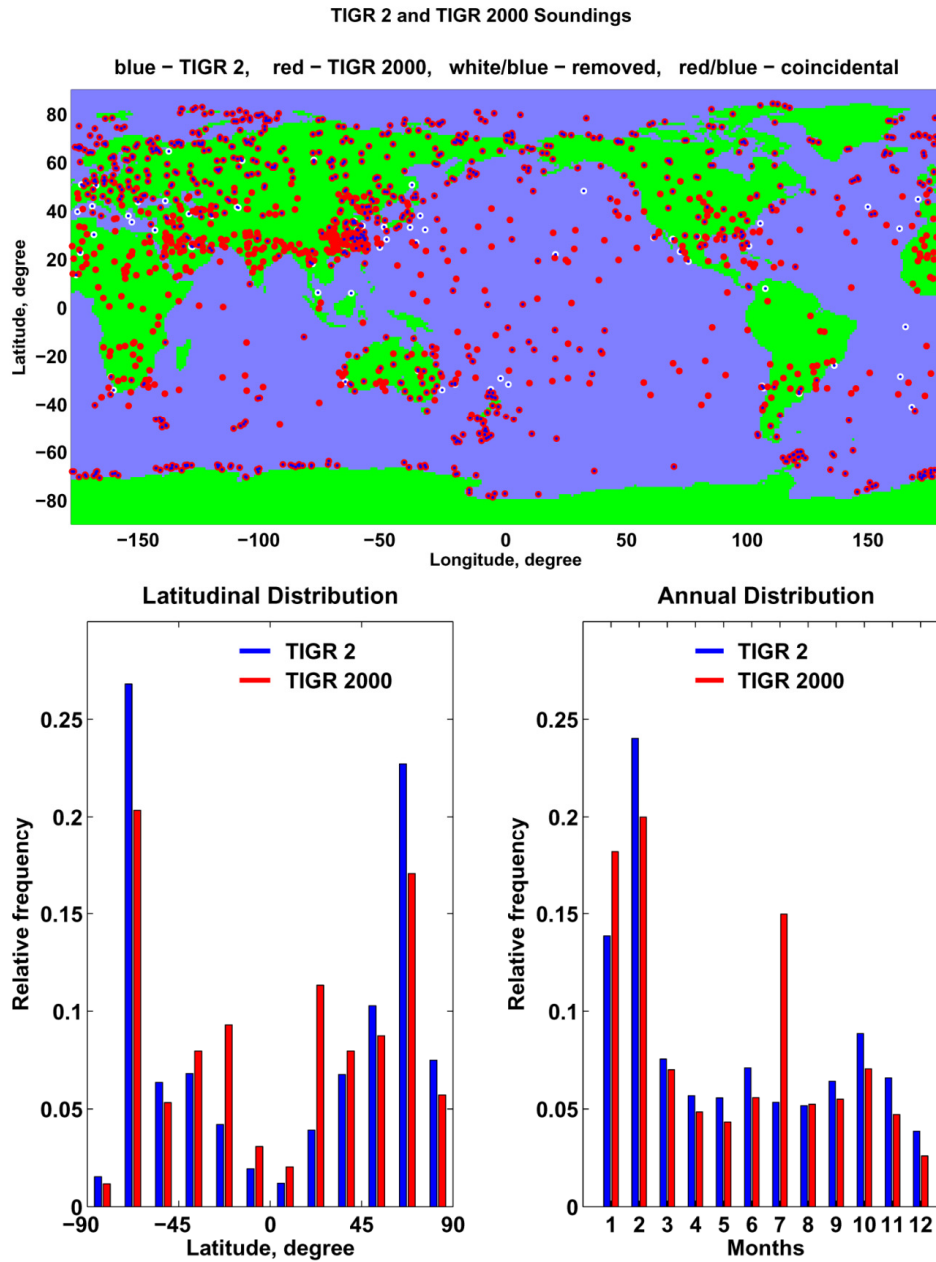
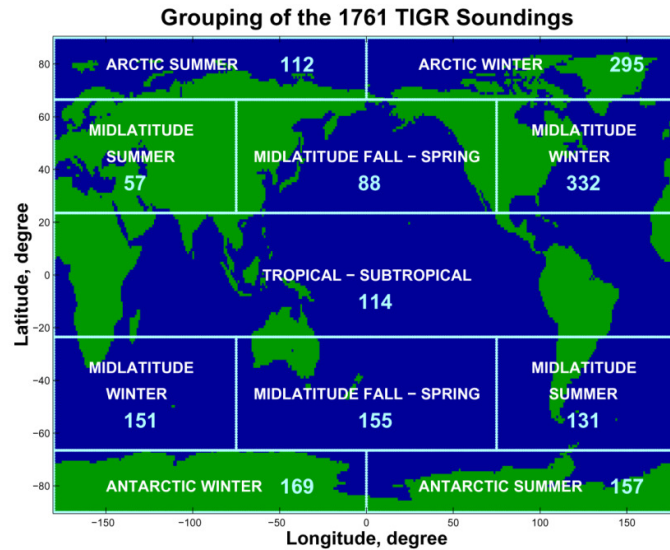


Figure 5. Latitudinal and seasonal grouping of the TIGR 2 soundings. In the selected subset 228 soundings were distributed among 11 groups having about 20 soundings in each group. Latitudinal and seasonal classes were established considering the solar climatic zones.



3. Observed Empirical Facts

In 2002 at the NASA Langley Research Center the first set of global scale high accuracy LBL flux optical depth and flux density computations for the Earth and Mars were completed. At this time it was clear that the well known - and widely used - semi-infinite opaque formulas ($S_A = OLR(1 + \tau_A)/2$ and $S_G = OLR(2 + \tau_A)/2$, where $S_A = \pi B(\tau_A)$ is the source function at the ground) cannot be used for semi-transparent atmospheres. Also the theoretically derived semi-transparent equation, $\pi B(\tau_A) = OLR/f$, was awaiting for empirical verification, see [6]. We were looking for flux density-optical depth relationships which could be used for reasonable surface temperature estimates from the satellite measured OLR s, and for the quantitative computation of the greenhouse factors. After the routine plots of the $\tau_A, T_A, S_U, S_T, E_D, E_U$, and OLR quantities five rather unusual relationships among the flux density components and optical thicknesses emerged. In Fig. 6 and 7 the computational results are plotted for the individual soundings. The presented relationships proved to be very stable they were satisfied even with the two most extreme TIGR 2 atmospheric structures (they are presented in Fig. 8). The tentative naming of the relationships reflects to some fundamental physical laws which they might be associated with.

Here the important point is that the presented relationships were not derived from some well known physical laws of nature, but were obtained from observations and computations using first principles. We should also emphasize that the newly discovered A-E relationships in Figs. 6-7 are not the results of some lucky coincidental profile selections from the TIGR 2 archive. In the last years we repeated the computations using the TIGR 2000 archive, the VIRS training data set, the NOAA R1 archive and hundreds of special atmospheric structures from different sources .

Figure 6. Observed radiative flux relations obtained from the TIGR 2 archive (upper four plots) and from the standard Martian profiles (lower four plots). In each plot the cross-hair and the number above it indicate the global average S_U . The linear correlation coefficients of the regression lines are also displayed.

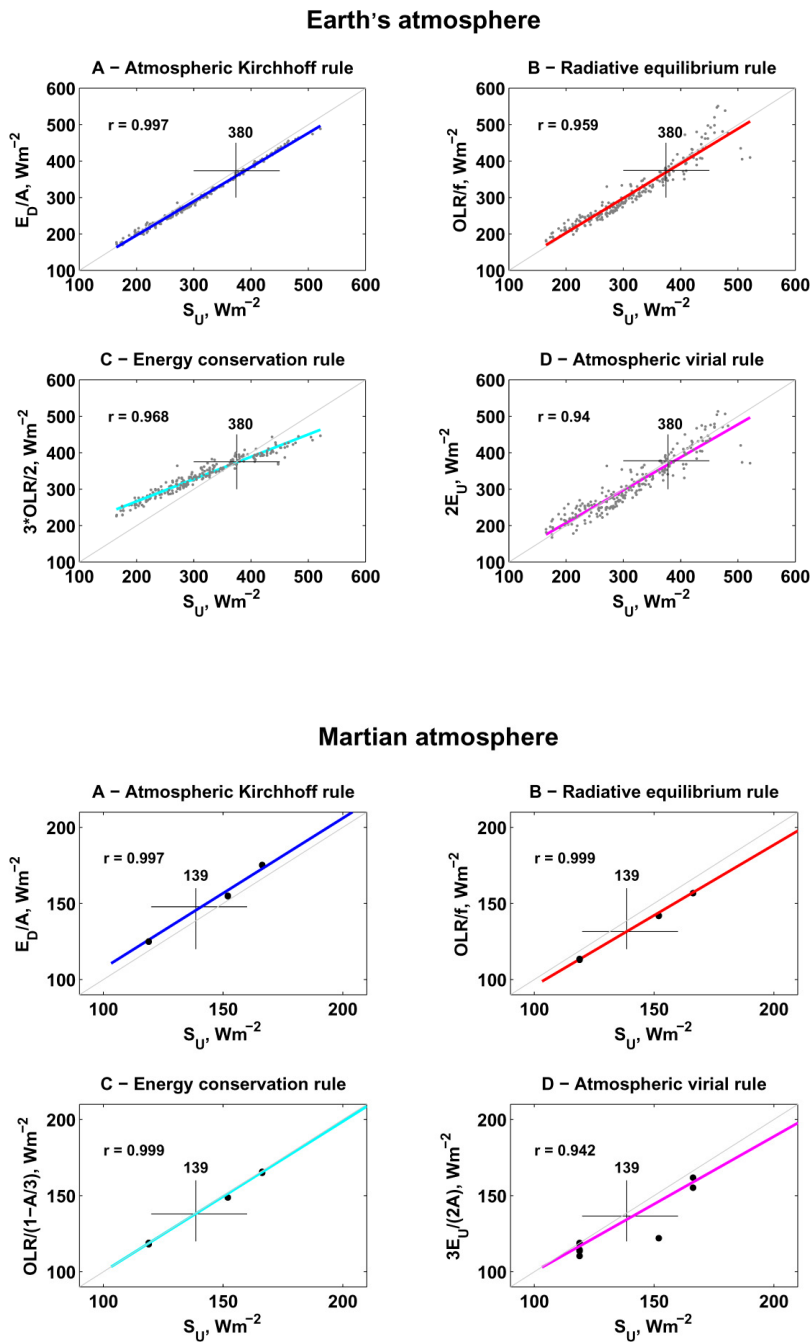
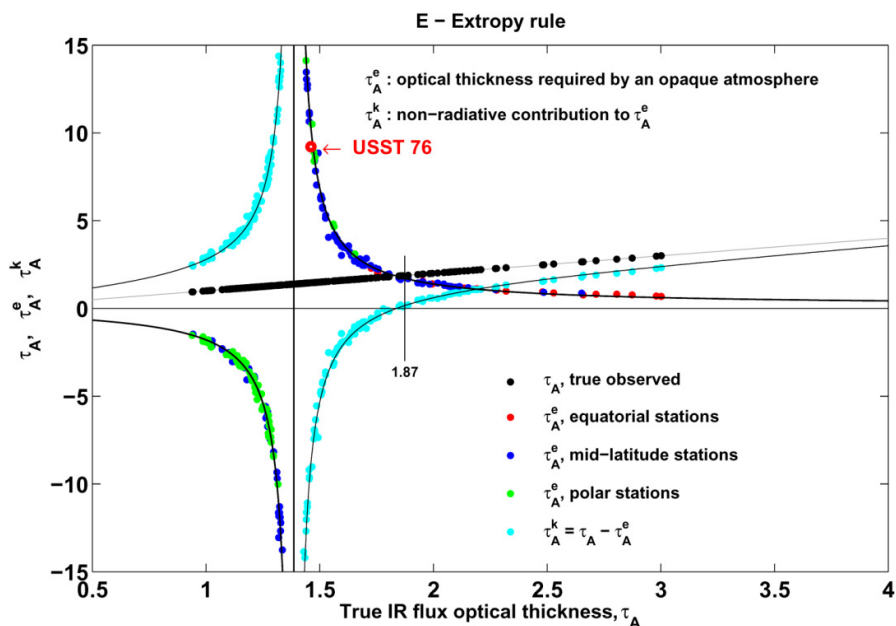


Figure 7. Virtual contributions of non-radiative fluxes to the observed true flux optical thickness in the Earth's atmosphere.



We could not find exceptions from the A-E rules. Even artificial structures like the USST 76 atmosphere fits in the picture, see the red arrow in Fig. 7. Judging from the correlation coefficients of the A-D plots in Fig. 6 none of the rules are perfect. In fact, tight fits in these type of relationships were not expected since the atmosphere is fundamentally a stochastic medium. Fig. 7 is different. Here the residuum correlation coefficient is practically 1.000 - the individual dots are sitting on the theoretical curve. We must conclude that the above rules represent real atmospheric radiative transfer properties and in order to get closer to the clue of the greenhouse effect one should try to explain and understand all of them.

Although in the recent study we focus on the IR fluxes at boundaries, further results are presented in Fig. 9 for the GAT vertical radiative structure. The radiative fluxes are plotted as the function of the layer geometrical thickness, z , measured from the top of the atmosphere ($z_{top} = 70$ km). In this computations a perfect blackbody radiator (cloud layer or ground surface) is assumed at the lower boundary. For some selected altitudes we present numerical data in Table 1.

The interesting features here are the following approximate equalities: $OLR(z_{2,2}) \approx E_D(z_{2,2})$, $E_D(z_0) \approx B(z_{2,2})$, $S_U(z_0) \approx E_D(z_0) + S_T(z_0)$, $OLR(z_{12,3}) \approx B(z_{12,3})$, and $E_D(z_{12,3}) \approx E_U(z_{12,3})$. At the indicated levels (see the subscripts of the altitude) the atmosphere has unique equilibrium states which are largely affect on the whole global energy balance picture. For example if the rule A is valid, then the $OLR(z_{2,2}) \approx E_D(z_{2,2})$ equation means that the global average atmosphere must be in equilibrium with a cloud layer at 2.2 km altitude. In other word, the cloud top and the atmosphere above should be

in radiative equilibrium with the global average all-sky $OLR^A \approx 236.5 \text{ Wm}^{-2}$. The last two equations imply that around 12.3 km altitude the atmospheric greenhouse effect stops, $G = S_U - OLR = 0$. The detailed analysis of the vertical structure of the IR radiation field will be the scope of another article.

Figure 8. Rare atmospheric situations. Extreme dry and cold and warm and humid atmospheric structures in the TIGR 2 data base.

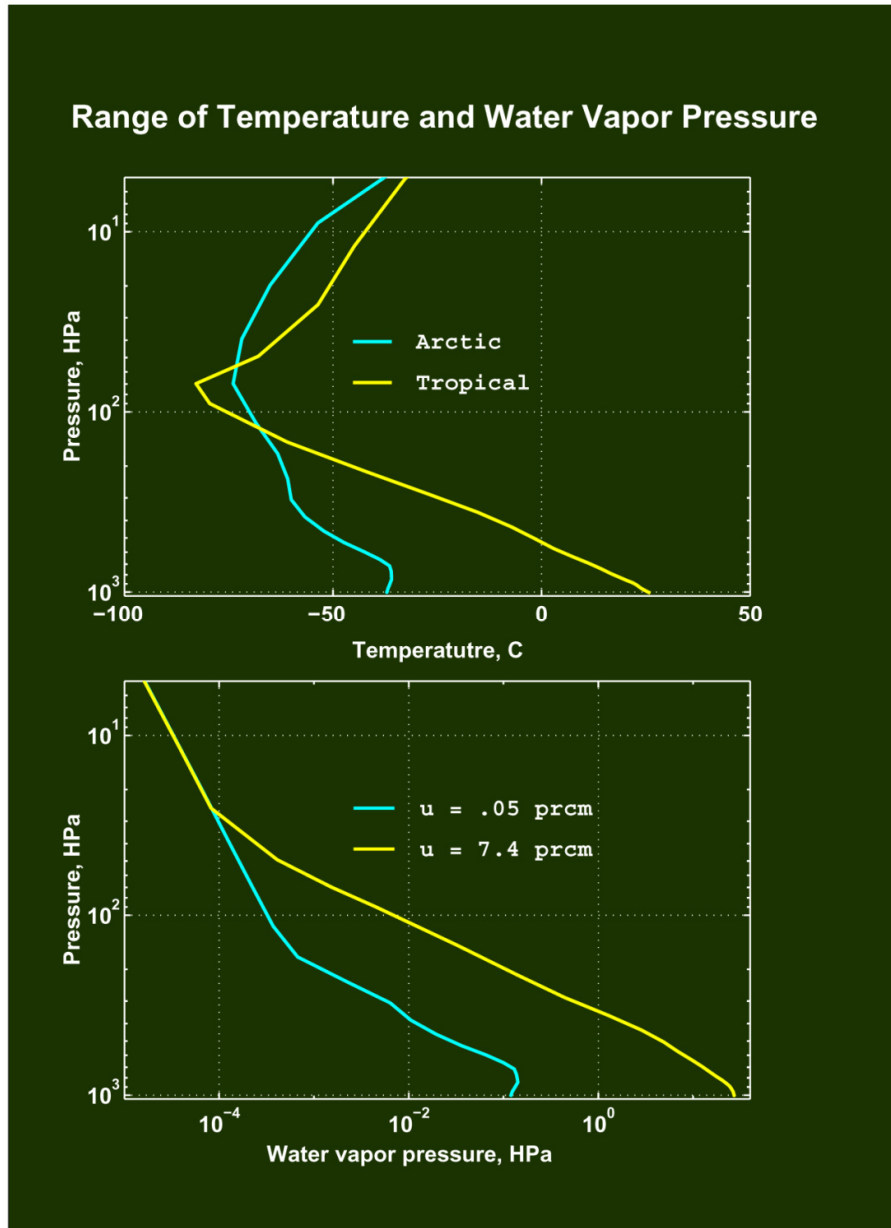


Figure 9. Radiative fluxes from an atmospheric layer bounded by the $z_1 = z_{top}$ and $z_2 = z$ altitudes.

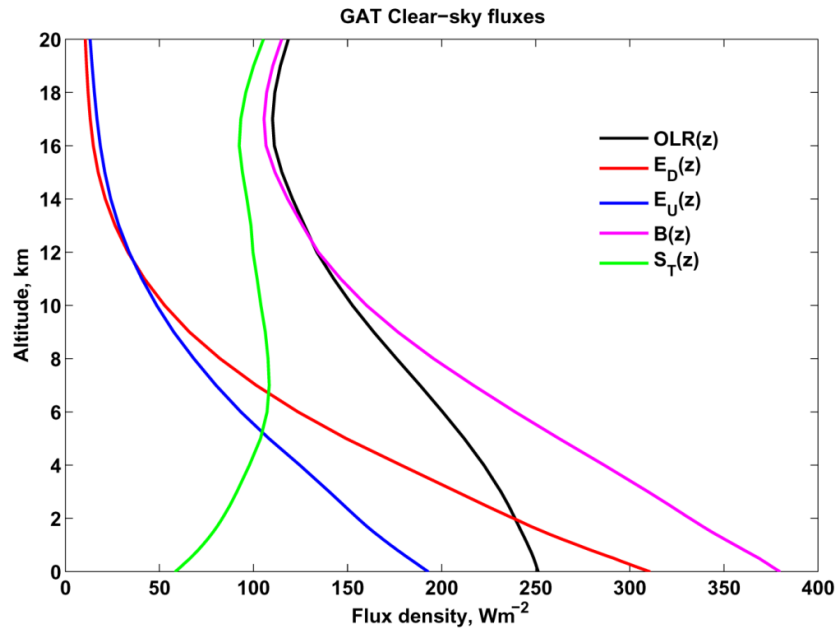


Table 1. Vertical radiative structure of the GAT atmosphere. Altitude is in km, fluxes are in Wm⁻², τ_A , T_A , and f are dimensionless.

Altitude	<i>OLR</i>	<i>E_D</i>	<i>E_U</i>	<i>B(z)</i>	<i>S_T</i>	<i>T_A</i>	τ_A	<i>f</i>
60.0	202.1	0.090	0.083	202.1	202.0	0.9995	0.0005	1.0000
38.4	221.1	2.38	2.38	220.9	218.7	0.9901	0.0100	1.0000
12.4	131.0	31.5	31.6	131.0	99.4	0.7587	0.2760	0.9829
12.3	131.4	32.0	32.0	131.5	99.3	0.7551	0.2809	0.9823
6.88	189.9	108.2	81.73	219.6	108.2	0.4936	0.7060	0.9092
5.24	209.3	148.8	104.6	256.8	104.6	0.4083	0.8957	0.8681
2.24	236.4	236.4	149.9	323.9	86.5	0.2670	1.3206	0.7729
0.00	251.2	323.8	192.7	379.6	58.5	0.1542	1.8693	0.6615

5. Theoretical Interpretations

The analytical equations representing the A, B, C, D, and E type relationships for the Earth in Figs. 6 and 7 may be summarized in the next five equations:

A: Atmospheric Kirchhoff rule:

$$E_D = A_A = S_U A = S_U (1 - T_A), \quad (3)$$

B: Radiative equilibrium rule:

$$S_U = OLR / f = OLR(1 + \tau_A + T_A) / 2 = OLR(2 + \tau_A - A) / 2, \quad (4)$$

C: Energy conservation rule:

$$S_U - OLR + E_D - E_U = OLR = F^o, \quad (5e)$$

D: Virial rule:

$$S_U = 2E_U, \quad (6e)$$

E: Extropy rule:

$$\tau_A = OLR / (S_U - 4S_T). \quad (7)$$

Eqs. (3-4,6e) appears to be valid for each individual soundings and also for the global averages, Eqs. (5,7) only valid for the global averages. In principle for the global averages any combinations of Eqs. (3-7) must hold. For the Martian atmosphere the energy conservation and virial rules taking different forms:

C: Energy conservation rule:

$$S_U - OLR + E_D - E_U = OLR - S_T = F^o - S_T, \quad (5m)$$

D: Virial rule:

$$S_U = 3E_U / (2A), \quad (6m)$$

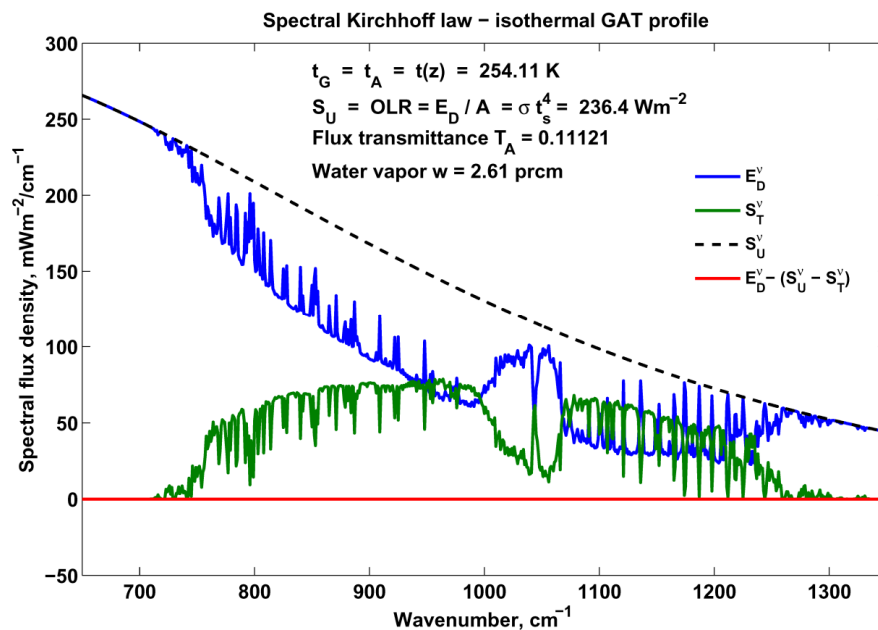
The reason of the above differences is in the different ways of the planetary redistribution of the absorbed solar radiation. In the next sections we shall discuss the above relationships with more details.

5.1. Atmospheric Kirchhoff Rule

Recently some researchers raised the question of the applicability of the Kirchhoff rule for atmospheric radiative processes, see for example [17]. Since in [6,9] the Kirchhoff law was not applied by any means, such critiques have not much scientific ground. Couple of hundred atmospheric structures show the $E_D \approx A_A$ relationship (with about 3% maximum deviations, as it is presented in Fig. 6 plot A), then the only way to refute this empirical fact is to show a structure which is not consistent with the Kirchhoff rule, or law. The different forms of the monochromatic, flux, directional etc. Kirchhoff law is well known in the general radiative transfer theory. It is also known that the classic monochromatic Kirchhoff law is not valid in the close vicinity of strong absorption/emission lines see Figs. 18-19 in [6]. It is also difficult to adopt this law for atmospheric IR flux densities where the inhomogeneous atmosphere is in permanent physical contact with a solid or liquid surface. The important finding here is the ability of any real atmosphere to instantly adjust its radiative structure to closely satisfy Eq. (3). The physical explanation is very simple. The relaxation time of the radiation field is much smaller than any other macroscopic heat or energy transfer processes (related to the

motion and thermodynamics) of the atmosphere. The vibrational-rotational relaxation time is in the order from 2×10^{-6} to 2×10^{-5} sec at 1 atm. and 200K. The IR radiation field is close to quasi-static equilibrium with the surrounding environment and it sees ‘instantly’ the whole atmosphere, independently of the dynamics of system. The strict validity of the spectral Kirchhoff law for a hypothetical isothermal atmosphere is trivial and exact. Such situation is presented in Fig. 10.

Figure 10. The spectral Kirchhoff law in isothermal atmosphere requires the following equalities: $OLR = S_U = E_D / A = E_U / A$, and $E_U / S_U = E_D / S_U = 1 - S_T / S_U = A$. Since $S_U = OLR / f$ and $S_U = E_D / A$ equations cannot be satisfied simultaneously, such an atmosphere can never be in radiative equilibrium, see [6,p24].



As we can conclude, the spectral Kirchhoff law is perfectly reproduced with HARTCODE, see the red line in Fig. 10. Similar, but spectral radiance simulations for isothermal atmospheres are routinely performed to test the numerical performance of LBL radiative transfer codes, see Kratz et al. [16,p332]. The HARTCODE computational accuracy for flux transmittance is excellent, $100(S_U - E_D / A) / S_U = 0.0000022 \%$.

The conditions of the stability of the thermal structure of an air column are also of interest. In Figs. 11 and 12 simulated global average flux transmittance, atmospheric downward emittance, and observed source function profiles are presented for clear and cloudy GAT atmospheres. In these simulations the cloud layer is represented by a perfect black surface at a given altitude with an infinitesimal vertical extension and in thermal equilibrium with the surrounding air. The thermal equilibrium and a perfectly black radiator also assumed at the ground surface ($S_U = \pi B(z_0)$ at zero altitude).

The question of the radiative exchange equilibrium (introduced in [9]) between the surface (or the lowest air layer) and a particular part of the atmosphere was also studied. In case if thermal inversions are present in the temperature profile, theoretically the surface must be in perfect radiative exchange equilibrium with those atmospheric layers having the same temperature. For this kind of computations we selected 42 inversion cases from the TIGR 2 data and computed the differences in the absorbed and emitted radiations in each layer. Such kind of tests are very useful because they can point to inconsistencies and programming bugs in the computational algorithms. In Figs. 13 and 14 the results of such type of computations are presented. Although these computations required substantial modifications in the HARTCODE output routines, to our satisfaction, our LBL code computed the layer net radiation according to the expectations.

We should note, that in case the global average atmosphere represents a long term average structure which is in an overall radiative balance with the surrounding space then the ~3% anisotropy effect in the Kirchhoff rule must be taken care of by an effective hemispheric emissivity factor of $\epsilon \approx 0.967$.

Figure 11. Clear-sky Kirchhoff law. The atmospheric downward emittance is equal to the atmospheric absorption of the surface upward radiation, $S_U = E_D / A$. The whole atmospheric column is in radiative equilibrium with the surface air. This is the obvious condition for the local thermodynamic equilibrium ,LTE, and the existence of a stable temperature profile. At higher altitudes this figure shows, that any emitting cloud layer is also in radiative equilibrium with the atmospheric column above. This is the condition of the LTE in the air column above the cloud layer.

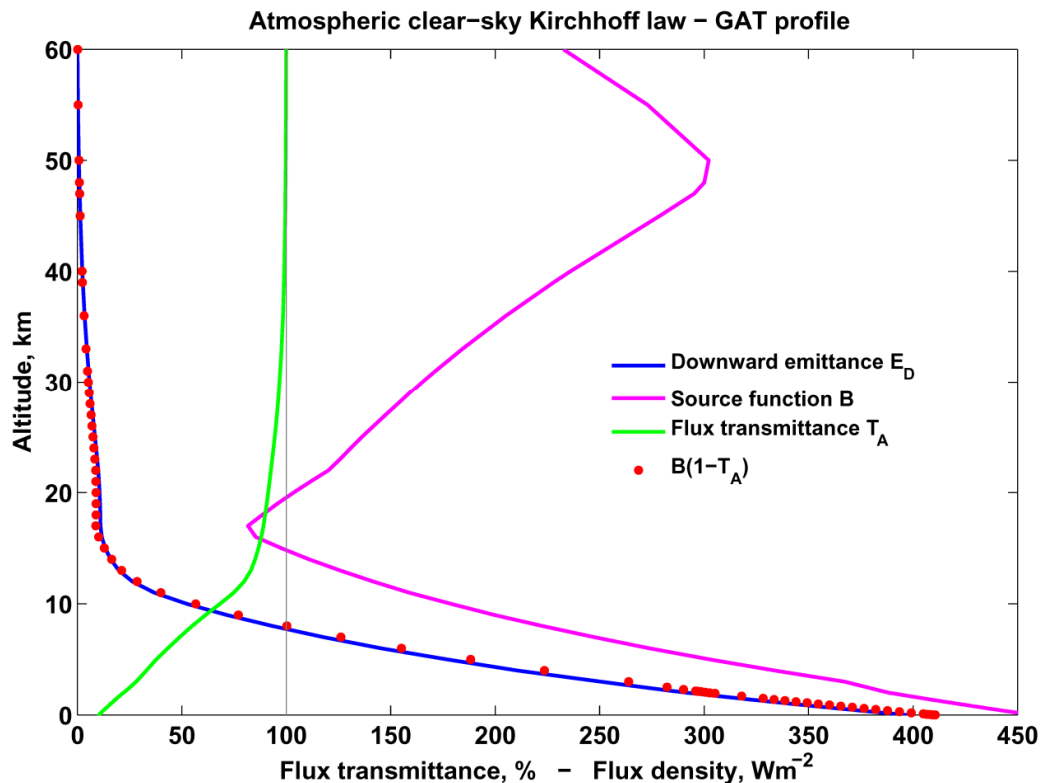


Figure 12. Cloudy-sky Kirchhoff law. Up to about 3 km altitude the mean atmospheric emittance is equal to the absorbed mean surface radiation (from ground and cloud bottom), T_M is the weighted average flux transmittance. Apparently the cloud layer is acting as a cavity, the atmosphere below the cloud layer is in radiative equilibrium with the emitting surfaces at the upper and lower boundaries.

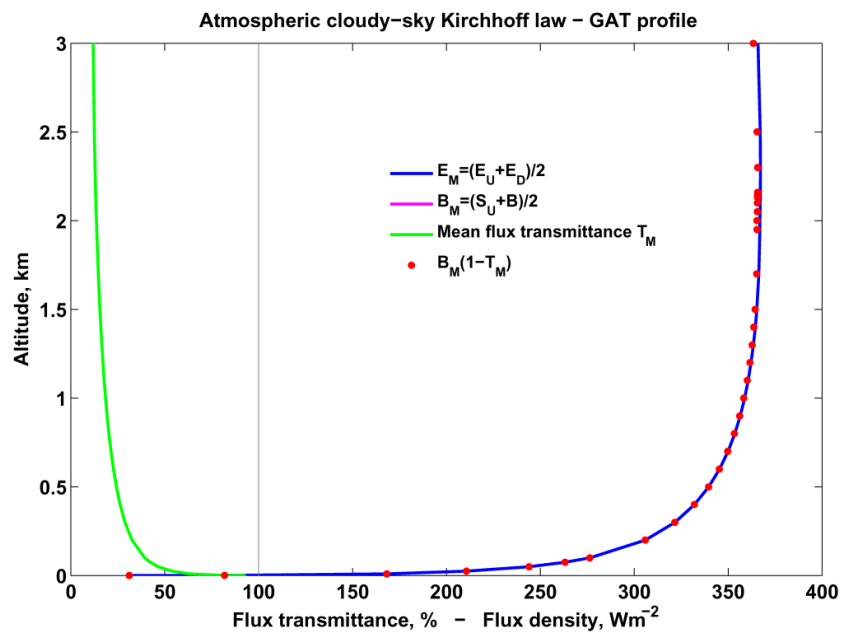


Figure 13. Low level temperature inversion and radiative exchange equilibrium. HARTCODE determined the equilibrium altitude using the yellow dots for interpolation. The accuracy of the equilibrium altitude is ~4 m

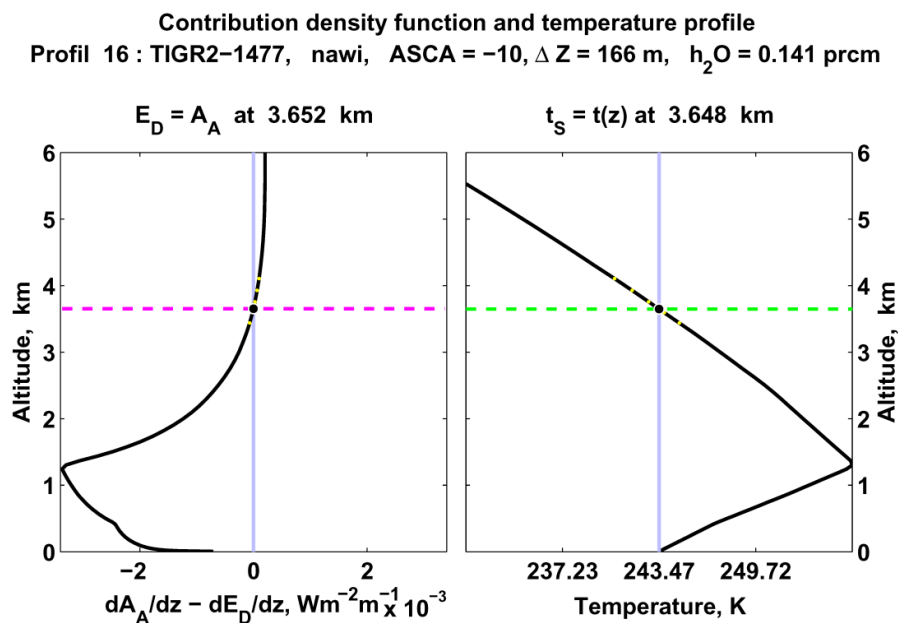
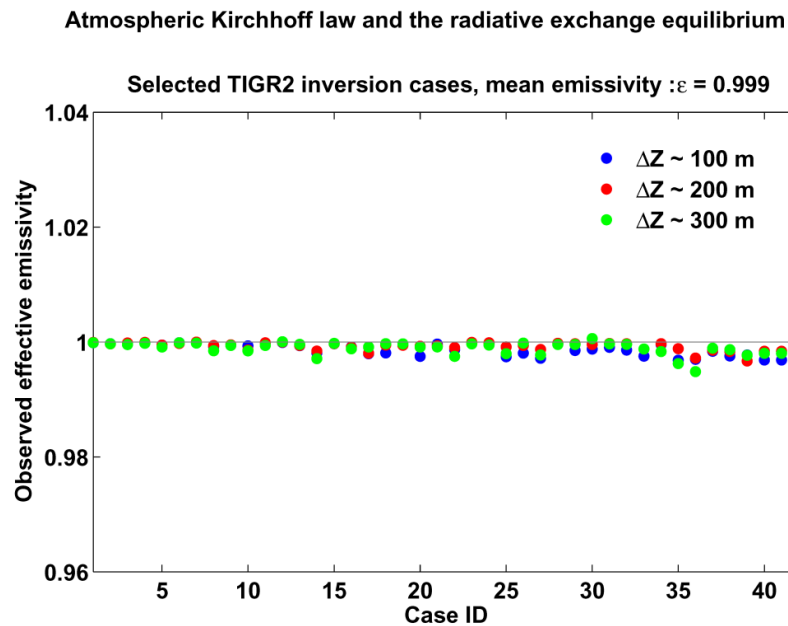


Figure 14. Emissivity estimates from temperature inversion cases. Different colors belongs to different ΔZ vertical resolutions. These results reproduce the $\varepsilon \approx 1.0$ expected surface emissivity with sufficient numerical accuracy.



5.2. Radiative Equilibrium Rule

In 2002 the only available theoretical relationship between the IR optical depth and the source function profile was the classic semi-infinite Eddington solution, and its corrected versions (which tried to resolve the surface temperature discontinuity problem). However, the related ‘linear in τ ’ equations for the semi-infinite atmosphere turned out to be mathematically incorrect, [6]. In our view the IR radiative structure of the atmosphere (the vertical distributions of B , E_D , E_U , and S_T flux densities) is driven by the vertical profile of the flux optical depth (or flux transmittance). Due to the monochromatic radiative equilibrium the integrated net monochromatic flux density profile is uniquely related to the vertical temperature (source function profile) and GHG distributions (flux optical depth profile). This relationship in a hydrostatic semi-transparent bounded atmosphere is expressed by the $S_U = OLR / f$ (Eq. 28 in [6]). This equation has dramatic consequences regarding the sensitivity of the atmosphere to GHG perturbations.

It is important to notice, that at the derivation of Eq. 4 the ‘gray approximation’ is applied only for the convenience of dropping the wave number index in the equations. In case of monochromatic flux densities we may write the solution in monochromatic form of : $f^v S_U^v = OLR^v$, where $f^v = f^v(\tau_A^v) = 2 / (1 + \tau_A^v + \exp(-\tau_A^v))$ is the monochromatic transfer function, and τ_A^v is the monochromatic flux optical depth. Integrating both sides with respect the wave number and applying the mean value theorem of the calculus one may easily arrive at Eq. 4.

The naming of ‘Radiative Equilibrium law’ is again quite straightforward. The new semi-transparent radiative equilibrium equations, the derivation of B_0 , $B(\tau)$ and the simple Eq. 4 from the well known original equilibrium relationships were proved with sufficient mathematical rigor, [6]. However, the use of radiation equilibrium terminology requires some clarification. The definition of the radiative equilibrium is given by $B(\bar{\tau}) = (3/4\pi)H\bar{\tau} + B_0$, where H is the Eddington flux, and B_0 is an integration constant. Once we have a linear (actual or equivalent) $B(\bar{\tau})$ source function profile with the required slope and B_0 then the atmosphere is said to be in radiative equilibrium. In such case the atmosphere has the proper amount of greenhouse gases (H₂O, CO₂, O₃ etc.) to support the $S_U = OLR/f$ relationship.

Note, that E_U implicitly involves all non-IR atmospheric processes, therefore it does not make any sense to talk about convection, turbulent mixing, advection or SW atmospheric absorption separately. Our immediate interest was to study the relationships between the radiative fluxes at the top and bottom boundaries of the atmosphere therefore we did not deal with the partition of E_U into its different components. One may call a true atmospheric thermal structure as radiative-convective equilibrium but this terminology is misleading. Instantaneous thermal structures are formed according to the stochastic mixing of the atmosphere which is governed by the energy minimum or entropy maximum principles (both on local and global scales).

5.3. Energy Conservation Rule

The energy conservation rule for the Earth (Eq. 5e), as it was mentioned already, valid only for the global average structure. The simple form of $S_U = 3OLR/2$ requires the validity of the $E_D = A_A$ relation and a general assumption about the dynamics of the system. The most plausible assumption is that the Earth, with its extremely complex dynamical system of virtually infinite degree of freedom, is able to maximize the $G = S_U - OLR$ greenhouse factor. This means that the entropy production of the radiation field, (the conversion of F_o into OLR) is happening with the maximum rate. Notice, that the G is not representing the absorbed surface upward radiation, (or according to some NASA greenhouse experts the ‘trapped’ IR radiation in the atmosphere), but it is the $t_G - t_E$ temperature difference that drives the atmospheric and oceanic circulation which re-distributes the absorbed SW radiation and by doing this it is the fundamental source of the thermodynamic entropy production of the system. Our proposition here is that the system can make use of the transmitted surface upward flux density by adding the atmospheric SW absorption (let us say F) to the surface energy balance by non radiative energy transfer. By this way independently of the magnitude of the S_T (that is lost to space) the total F_o may contribute to the thermodynamic entropy production of the system. Obviously the overall energy balance of the system cannot be violated, therefore the $S_T = F$ relation must hold. This is why Eq. 5e was named to energy conservation rule. Applying the $S_U - OLR = E_D - E_U$ equality (a consequence of the Kirchhoff rule) one may readily obtain the $S_U = 3OLR/2$ form of the energy conservation rule.

The energy conservation rule for the Mars is (Eq. 5m). In this case Eq. 5m expresses the fact that the Martian atmosphere has little dynamics (no clouds, no ocean currents and strong atmospheric circulation) therefore nothing can compensate for the relatively large amount of surface transmitted flux density which - instead of contributing to the entropy production - is lost to space. Applying the Kirchhoff rule Eq. 5m takes the simple $S_U + S_T / 2 = 3OLR / 2$. Some more details about the Martian greenhouse effect can be found in [6].

5.4. Virial Rule

Unfortunately climate scientists tend to forget about the virial theorem and they usually rendering it unusable for climate research. Some of them openly spreading their belief that in atmospheric physics the virial concept is useless and it is a serious mistake to apply, see De Bruin [17] or V. Toth [18]. Publishing this kind of views is not very much in the interest of the atmospheric science. According to Chandrasekhar, [19] the virial theorem can take the next forms: $2T + \Omega = 0$, or $3(\gamma - 1)U + \Omega = 0$, where T is the mean kinetic energy, Ω is the gravitational potential energy, γ is the specific heat ratio and U is the internal energy of the (bounded) system. Cox and Giuli, [20] states that: The virial theorem may be expressed in a variety of different forms and also may be interpreted in a number of different ways. It should be pointed out that the virial theorem need not necessarily apply to the entire system, but may apply to only a part of the system. Further on from Satosh, [21] we can learn, that: A simple relation holds between potential energy and the internal energy under hydrostatic balance. This relation is a special case of the virial theorem.

Our virial rules $S_U = 2E_U$, Eqs. 6e, and $S_U = 3E_U / 2A$, Eq. 6m, are relationships between the surface upward flux density and atmospheric upward emittance. One has to note, that in the case of the Martian atmosphere the surface upward flux density depends also on the atmospheric IR absorption. It is also a well known and observed fact, that the Martian atmosphere has a diurnal change in the surface pressure that is, in the atmospheric mass. From astrophysics we also know that - according to the Vogt-Russel theorem - there must be a relationship between the mass of the star and the luminosity of the star. Since at that time we did not have the $E_U = S_U(f - T_A)$ relationship (which is a version of the radiative equilibrium rule), the above facts gave us enough inspiration to give a try to relate E_U to the surface pressure or to the mass of the Earth. The computations for the TIGR 2 archive are presented in Fig. 15. It is quite obvious that the virial theorem is applicable for the Earth's atmosphere and represent a permanent constraint on the IR radiation field.

5.5. Exentropy Rule

The exentropy equation, Eq. 7, was one of the first relationships that suggested a numerical estimate for the true global average IR optical thickness of the atmosphere relying only on an assumption on the dynamics of the system. The exentropy as a measure of the maximum entropy production state in non-equilibrium (dissipative) systems was introduced by Martínás, K., [22] and Gaveau, B., Martínás, K., Moreau, M. and Tóth, J., [23]. The stochastic nature of the global humidity field and global cloud

cover suggested that the local instantaneous *OLR* may only depend on an effective instantaneous optical depth, τ_A^e , of the atmosphere which is governed by the local instantaneous irreversible non-

Figure 15. Virial concept - hydrostatic atmosphere. Internal energy is computed with one degree of freedom. Gravitational potential energy is referenced to the surface.

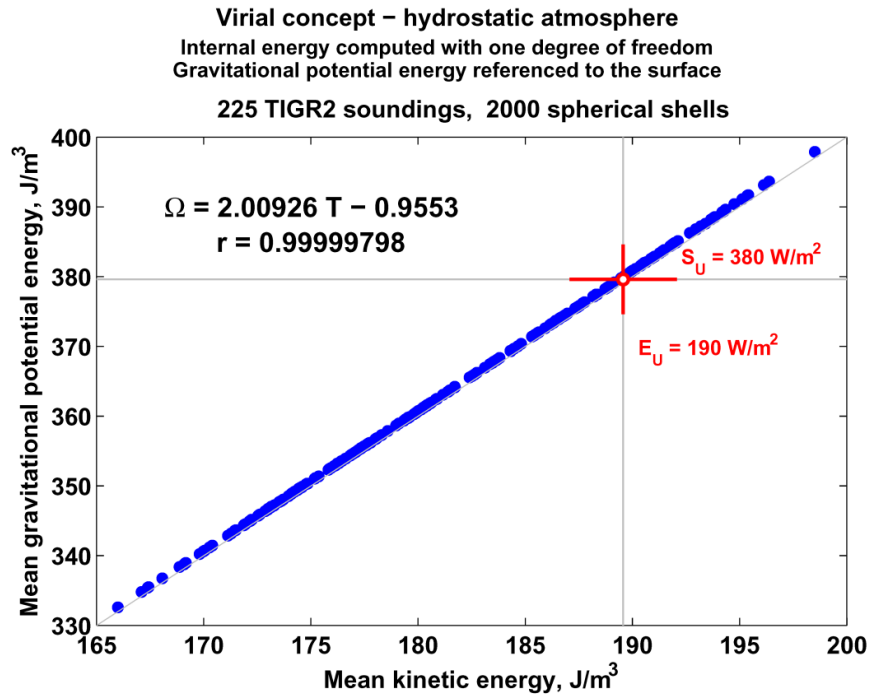
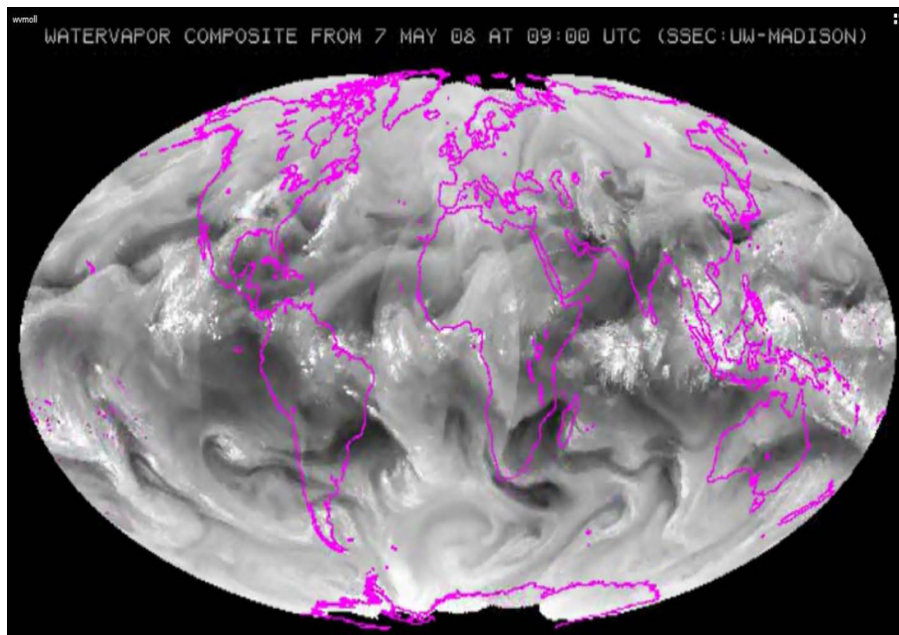


Figure 16. Satellite observed stochastic nature of the atmospheric humidity field. This picture is a snapshot from a ten day video-record prepared by McIDAS, SSEC, University of Wisconsin, Madison.



radiative energy flow within the system. As such τ_A^e could be regarded as the scalar entropy of the Earth-Atmosphere system. Since the net non-radiative energy flow in the system (in global energy balance, $OLR = F^o$) must sum up to zero, it is expected that the system configures itself in such a way that the global average $\bar{\tau}_A^e = \bar{\tau}_A$ and the individual τ_A^e has no correlation with any IR flux related variables. The turbulent mixing of the humidity field is demonstrated in Fig. 16. The mathematical derivation of Eq. 7 is straightforward: we assume that the effective surface temperature of an infinite opaque atmosphere is proportional with product of τ_A^e and the atmospheric upward emissivity E_U : $\tau_A^e E_U = OLR(1 + \tau_A^e)/2$. This leads to a transcendental equation for τ_A^e which has the $\tau_A^e = 1.837 \approx \tau_A = 1.867$ solution for the global average and has no correlation with any other IR radiative transfer related variables. Eq. 7 is a version of the $\tau_A^e E_U = OLR(1 + \tau_A^e)/2$ equation.

6. Results and Discussion

Before going into the details of the physical meaning of the rules presented in Fig. 6 we should spend some more time with the energy conservation and virial rules (Eqs.5e,6e). Unfortunately this two equations do not satisfy an obvious and necessary physical condition which is sometimes called as the transparent limit constraint. For a transparent atmosphere, $\tau_A = 0$, and the $S_U = S_T = OLR$ and $E_D = E_U = 0$ conditions should be satisfied.

For the above purpose in [6] we introduced the $S_V = S_T/2 - E_D/10$ virial term. Adding S_V to the left hand side of Eq. 5e, we obtain an equation which obeys the transparent limit, and satisfies both of the original equations. It is easy to show that Eqs. 5e and 6e can be trivially satisfied with $S_T/S_U = 1/6$: $S_U = 2E_U = 2OLR - 2S_T = 2(2S_U/3) - 2S_T$, from which follows $S_U = 6S_T$. The equivalent form of this (using the observed $E_D = A_A$ empirical fact) is $S_T - E_D/5 = 0$. We assume the general equation in the form of $S_U + S_V = 3OLR/2$, where $S_V = X(S_T - 5E_D)$ and X is a non-zero multiplier. In the transparent atmosphere limit (no absorbers and no clouds) $S_U + XS_U = 3S_U/2$ from which $X = 1/2$, and $S_V = S_T/2 - E_D/10$. The final form is $S_U + S_T/2 - E_D/10 = 3OLR/2$ which can be reshaped into a much simpler form:

$$S_U = 5OLR/(3 + 2T_A). \tag{8}$$

Now we are interested in the conditions when all of the four empirical relationships and the related Eqs. 4 and 8 are simultaneously satisfied. Since we are left with only one variable as unknown, (τ_A), and two relatively simple equations the solution for τ_A may be obtained easily from the next transcendental equation:

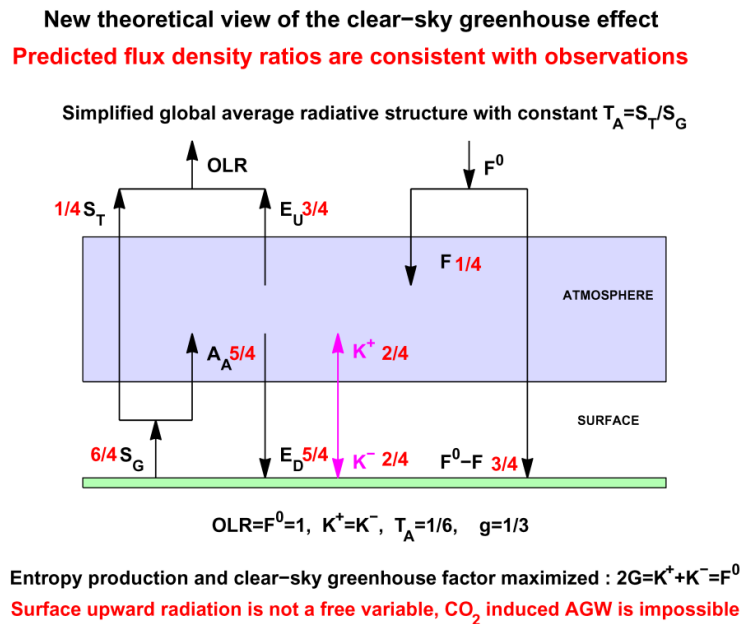
$$g = 2A/5. \tag{9}$$

The big problem for NASA, IPCC and other AGW promoters starts here. The solution of Eq. 9 is:

$$\tau_A = 1.867, \tag{10}$$

and this unique optical thickness does not depend on any particular GHG concentration. If this is true and $\tau_A = 1.867$ is scientifically verified by further observations then the AGW madness is over. The atmosphere takes care of its absorption properties and humans can not alter it. This theoretical result does not mean, that the planet cannot warm or cool because of the changes in other factors, but the CO₂ greenhouse effect is excluded from the probably rather long list of other candidates. A model of a quasi-static stable climate with constant T_A and τ_A is presented in Fig. 17.

Figure 17. Steady-state climate model with constant true IR optical thickness. Global warming is only possible through SW albedo changes, SW solar input to the system or changes in the effective IR emissivity.



The first verification of the $\tau_A = 1.87$ equilibrium optical thickness was based on the TIGR 2 and NOAA radiosonde archives. Results are summarized in Fig. 18. All annual mean optical depth data support Eq. 10. In Fig.19 Theoretical normalized flux density components are plotted. The gray dots are the observed E_U/S_U ratios. The global averages are again supporting Eq. 10. In Fig. 20 we present comparisons with other authors who had published IR flux densities or global average atmospheric structures. The main point here is the fact that apparently only the GAT structure is consistent with the tested theoretical relationships. If theory is correct then the global average atmosphere must have only one τ_A .

Figure 18. TIGR 2 and NOAA profiles. The red dots representing 61 annual mean profiles, (not resolved sufficiently to see the individual soundings). The theoretical $\tau_A = 1.867$ is fully supported.

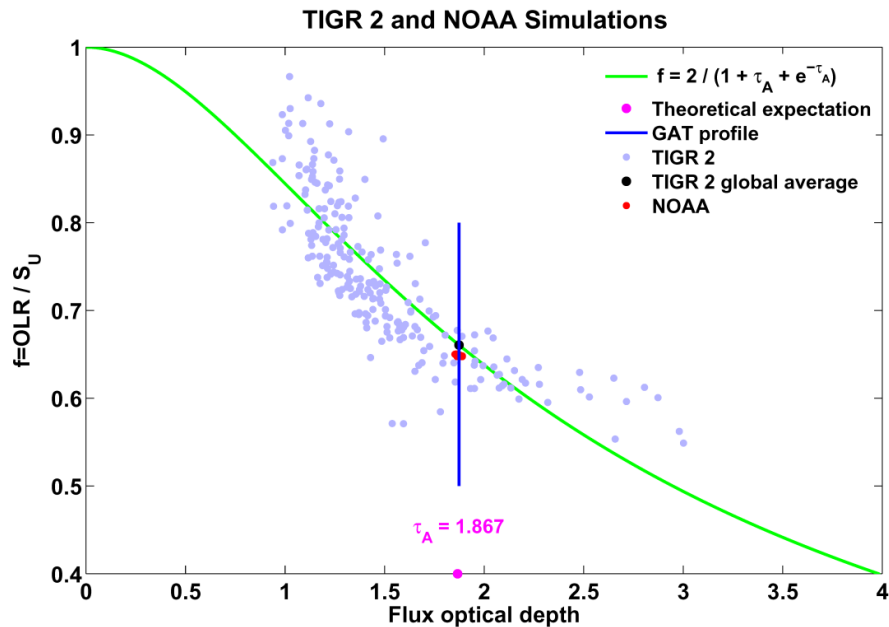


Figure 19. Normalized flux densities and annual mean TIGR 2 and NOAA optical thicknesses. Note that the thin magenta line of E_U/S_U is very close to 0.5 therefore competing with the $S_U = 2E_U$ virial rule. Again, the theoretical $\tau_A = 1.867$ is fully supported.

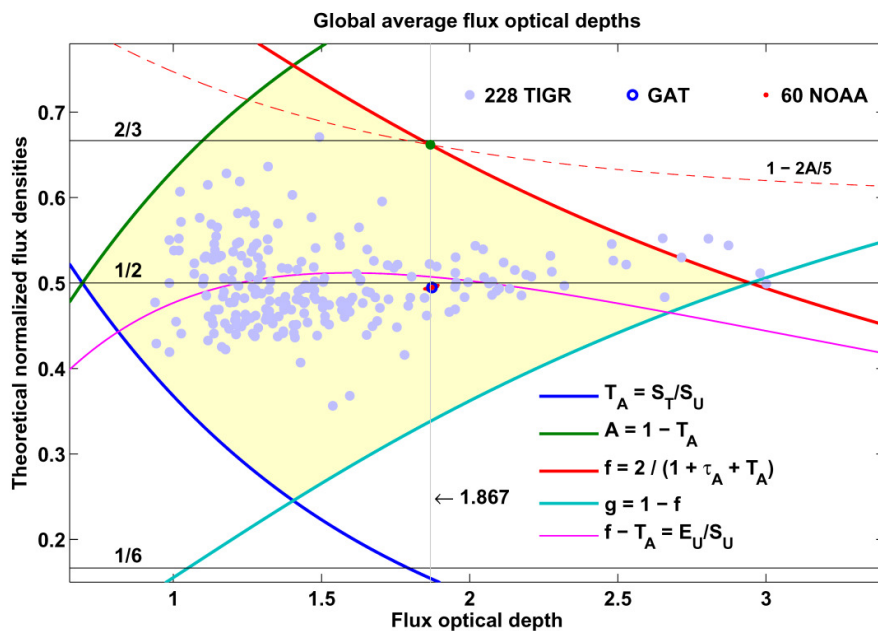


Figure 20. Comparisons of different global average flux estimates and their compatibility with the theoretical expectations. Except from the GAT profile none of them a suitable for global energy budget studies. The worst is the 1976 Kiehl-Trenberth budget. Unfortunately IPCC endorsed this budget. Here the GAT fully supports theoretical $\tau_A = 1.867$.

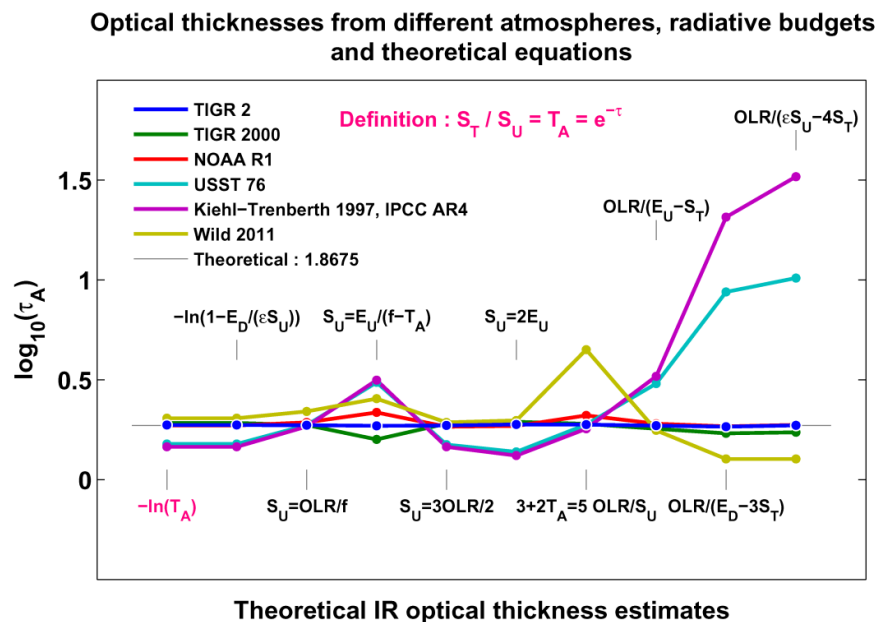


Figure 21. Atmospheric absorption trends in the last 61 years. The expected increase in the atmospheric absorption due to the ~21% CO₂ increase during this time period is not present.

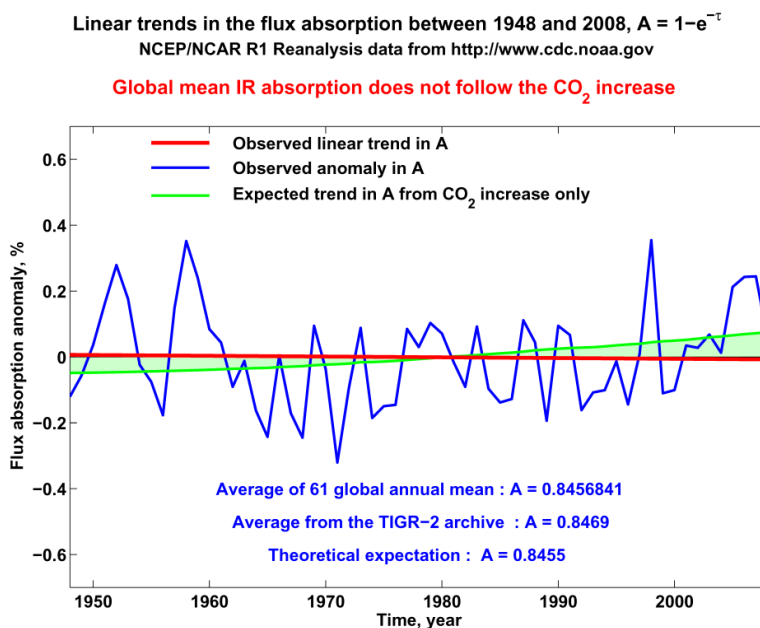


Figure 22. Optical thickness computations for different sub-sets of the NCEP/NCAR R1 archive. Short term fluctuations are not related to CO₂ increase. No τ_A trend in the data.

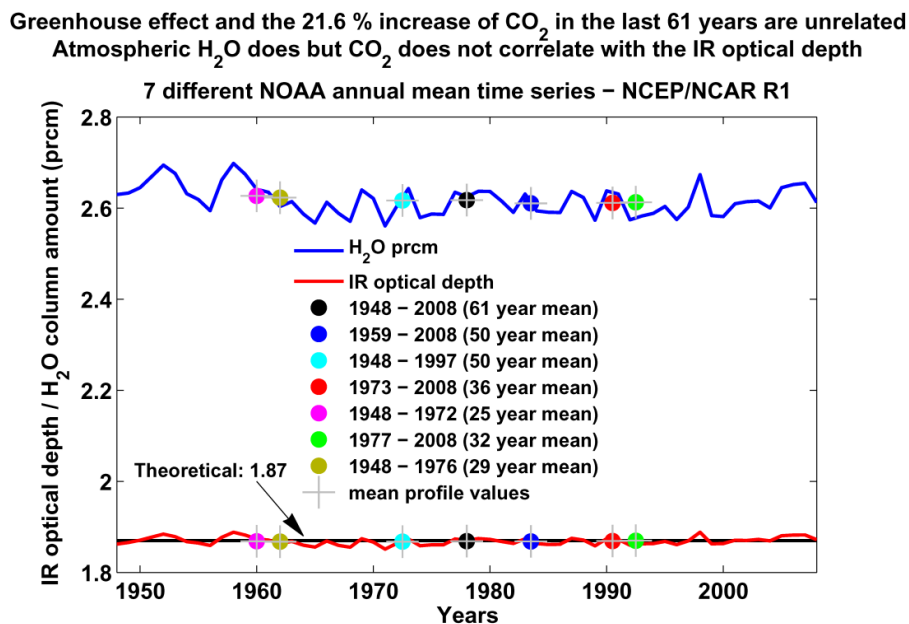


Figure 23. Numerical summary of the investigated sub-sets presented in Fig. 22. From the last two columns one may conclude that the CO₂ does not have the slightest effect on the true IR optical thickness of the atmosphere. Therefore the CO₂ greenhouse effect based AGW is non-existing, it is a scientific nonsense.

**NOAA NCEP/NCAR R1
Trendline correlation coefficient summary**

Time period	Centre Years	Altitude	Temperature	H ₂ O	CO ₂	Tau	
1948–2008	1978	61	0.7931	0.8183	-0.2841	0.9839	0.06488
1959–2008	1983.5	50	0.8059	0.8349	0.04499	0.9937	0.2976
1948–1997	1972.5	50	0.6621	0.6625	-0.4843	0.9827	-0.2284
1973–2008	1990.5	36	0.6947	0.7987	0.1148	0.9974	0.3491
1948–1972	1960	25	-0.005748	0.1731	-0.5907	0.983	-0.4184
1977–2008	1992.5	32	0.58	0.7424	0.03992	0.9973	0.267
1948–1976	1962	29	0.001769	0.0584	-0.6048	0.9804	-0.4396

**IR optical depth has no correlation with time.
The strong CO₂ signal in any time series is not present in the
in the IR optical depth data.**

In the last three figures (Figs. 21-23) the results of the search for long term optical depth trends in the 61 year long (1948-2008) NOAA NCEP/NCAR R1 reanalysis dataset are presented. Our attempts to identify any significant changes in the absorption characteristics of the atmosphere were unsuccessful. For the above tasks HARTCODE was pushed to extreme numerical accuracy, test runs for small optical depth perturbations are presented in [9]. In Fig. 21 the actual and expected atmospheric absorption trends are compared for the full time period. No change in the IR absorption was detected. In Fig. 22 the study was extended for six more sub-sets of the 61 year time period. The theoretical expectation in each sub-set was met, no changes in the $\tau_A = 1.87$ was apparent. In the last figure (Fig. 22) numerical data are presented about the trend computations in Fig. 21.

7. Conclusions

It is amazing that the global warming community and GCM modelers could debate CO₂ greenhouse effect based AGW issues for decades without having the slightest knowledge about the true IR atmospheric absorption and the related physical laws. According to the simple-minded or 'classic' view of the greenhouse effect the global average greenhouse temperature change may be estimated by the direct application of the Beer-Lambert law moderated by some local or regional scale weather phenomenon (R. Pierrehumbert, [2], A. Lacis, [1], A. P. Smith, [24], H. deBruin, [17], J. Abraham et al., [25]). This is not true. If the τ_A constant, then there is no AGW, there is no climate sensitivity and there is no H₂O feedback of any kind. All non-radiative atmospheric processes are contributing to one overall purpose, namely to keep the extropy (τ_A) constant and convert as much SW radiation to LW radiation as possible while maintaining the radiative energy balance and the minimum gravitational potential energy.

The dynamics of the greenhouse effect depend on the dynamics of the absorbed solar radiation and the space-time distribution of the atmospheric humidity. The global distribution of the IR optical thickness is fundamentally stochastic. The instantaneous effective values are governed by the turbulent mixing of H₂O in the air and the global (meridional) redistribution of the thermal energy resulted from the general (atmospheric and oceanic) circulation.

Greenhouse effect is a global scale radiative phenomenon and cannot be discussed without the explicit quantitative knowledge of the global characteristics of the IR atmospheric absorption and its governing physical principles.

Acknowledgements

I am very grateful for the help and support obtained from K. Gregory (Friends of Science Society) and Christopher Game (Lavoisier Group). Without their computational assistance this research project could not exist. Further on, I wish to thank D. Hagen and S. Welchenbach for their continuous attention and valuable advices.

References and Notes

1. Lacis, A.; Schmidt, G.A.; Rind, D.; Ruedy, R.A. Atmospheric CO₂: Principal Control Knob Governing Earth's Temperature. *Science* 2010, 356-359 www.sciencemag.org
2. Pierrehumbert, R.T.; Infrared radiation and planetary temperature. *Physics Today* Jan. 2011
3. Kiehl, J.T.; Trenberth, K.E. Earth's Annual Global Mean Energy Budget. *Bulletin of the American Meteorological Society* 1997, 78(2), 197-208
4. Trenberth, K.E.; Fasullo, J.T.; Kiehl, J. Earth's Global Mean Energy Budget. *Bulletin of the American Meteorological Society* 2009, March, 311-323
5. ERBE Monthly Scanner Data Product. NASA Langley Research Center, Langley DAAC User and Data Services 2004, userserv@eosdis.larc.nasa.gov
6. Miskolczi, F.M. Greenhouse effect in Semi-transparent Planetary Atmospheres. *Idojaras Quarterly Journal of the Hungarian Meteorological Service* 2007, 111(1), 1-40.
7. Miskolczi, F. M. High Resolution Atmospheric Radiative Transfer Code (HARTCODE) Technical Report. IMGA-CNR, Modena, Italy, 1989
8. Miskolczi, F. M.; Mlynczak, M. G. The Greenhouse Effect and the Spectral Decomposition of the Clear-Sky Terrestrial Radiation. *Idojaras Quarterly Journal of the Hungarian Meteorological Service* 2004, 108(4) 209-251
9. Miskolczi, F.M.; The stable stationary value of the earth's global average atmospheric Planck-weighted greenhouse-gas optical thickness. *Energy & Environment* 2010, Volume 21. No. 4
10. NOAA NCEP/NCAR Reanalysis data time series 2008, <http://www.cdc.noaa.gov>
11. Chedin, A.; Scott, N.A. The Improved Initialization Inversion Procedure (3I), 1983, Laboratoire de meteorologie dynamique, Centre National de la Recherche Scientifique, Note Interne LMD, No. 117
12. Ramanathan, V.; Inamdar, A.K. The radiative forcing due to clouds and water vapor. *Frontiers*

- of Climate Modeling Eds. J.T. Kiehl and V. Ramanathan; Cambridge University Press, 2006
13. Pierrehumbert, R.T. Principles of Planetary Climate. Cambridge University Press, 2010
 14. HITRAN2K, 2002, <http://cfa-www.harvard.edu/HITRAN/hitrandata>
 15. TIGR Thermodynamic Initial Guess Retrieval 2000 <http://ara.lmd.polytechnique.fr/htdocs-public/products/TIGR/TIGR.html>
 16. Kratz, D.P.; Mlynczak, M.G.; Mertens, C.J. Brindley, H.; Gordley, L.L.; Martin-Torres, J.; Miskolczi, F.M.; Turner, D.D. An Inter-Comparison of Far-Infrared Line-by-Line Radiative Transfer Models. *Journal of Quantitative Spectroscopy and Radiative Transfer* 2005, *90*, 323-341
 17. de Bruin, H.A.R.; Comments on "Greenhouse effect in semi-transparent planetary atmospheres" by Ferenc M. Miskolczi. *Idojaras Quarterly Journal of the Hungarian Meteorological Service* Vol.114, No. 4, October-December 2010, 319-324
 18. Toth, V.; The virial theorem and planetary atmospheres. *Idojaras Quarterly Journal of the Hungarian Meteorological Service* Vol.114, No. 3, July-September 2010, 229-234
 19. Chandrasekhar, S.; An Introduction to the Study of Stellar Structure. 1957 51-53, Eqs. 92 and 97, Dover Publications, 2010
 20. Cox and Giuli; Principles of Stellar Structures, 1968 page 408
 21. Satosh; Circulation Dynamics and GCMs.2004 page 331
 22. Martinás, K.; World Futures. 1997 50,483
 23. Gaveau, B.; Martinás, K.; Moreau, M.; Tóth, J. *PHYSICA*. 2002 A 305, 445
 24. Smith, A.P.; Proof of the Atmospheric Greenhouse Effect. *Physics.a0-ph*, February, 2008
 25. Abraham, J. et al.; Letter: To the Members of the U.S. House of Representatives and the U.S. Senate. January, 2011 <http://thehill.com>